Biological Journal of the Linnean Society, 2009, **97**, 413–426. With 7 figures

An unexpectedly sophisticated, V-shaped spermatozoon in Demospongiae (Porifera): reproductive and evolutionary implications

ANA RIESGO and MANUEL MALDONADO*

Department of Marine Ecology, Centro de Estudios Avanzados de Blanes (CSIC), Acceso Cala St. Francesc 14, Blanes E-17300, Girona, Spain

Received 4 November 2008; accepted for publication 22 November 2008

The demosponge *Crambe crambe* shows a peculiar spermatogenesis, hard to be reconciled with the basal position of sponges in the animal phylogeny. Early spermatogenesis stages showed most of the simple features expected in sponges. However, spermiogenesis departed from the anticipated process. Spermatids lengthened remarkably, forming a deep cytoplasmic pit around the cilium insertion, with the proximal axoneme bending to produce a V-shaped spermatozoon surprisingly similar to that known in the phylum Phoronida. The cytology was unexpectedly complex, with a needle-like nucleus of helically condensed chromatin, a conical acrosome with a subacrosomal rod, and a mitochondrion connected to the basal body by striated rootlets. These findings establish that the spermatozoon of broad-casting demosponges occurs in two structural categories ('primitive' and 'modified' type). This dualistic condition must necessarily have pre-dated the evolutionary apparition of higher metazoans, if we are to keep regarding sponges as the most primitive animals. We hypothesize that internal fertilization in *C. crambe* – and incidentally other demosponges – may depart from the general model assumed for spermcasting sponges. The V-shape of this spermatozoon suggests a design to favour autonomous penetration through the dense mesohyl to reach the oocytes, rather than engulfment and transportation by carrier cells towards the oocyte. © 2009 The Linnean Society of London, *Biological Journal of the Linnean Society*, 2009, **97**, 413–426.

ADDITIONAL KEYWORDS: early metazoans – entaquaspermatozoon – fertilization – gametic biology – gamete evolution – invertebrate reproduction – Phoronidea – spermatogenesis – sponges – striated rootlets.

INTRODUCTION

Many attempts have been made to classify the various degrees of morphological complexity shown by animal spermatozoa and to unravel the putative phylogenetic signal contained in their ultrastructure (e.g. Franzén, 1970; Afzelius, 1979; Baccetti, 1979; Reunov, 2001, 2005). The archetype of 'classical primitive' sperm (*sensu* Franzén, 1996; Reunov, 2005) has usually been described as a round cell propelled forward by an undulating posterior cilium [note that we use the term cilia to refer to eukaryotic organelles whose structure is characterized by an essentially identical arrangement of microtubules. Following Nielsen (2001) and Maldonado (2004), this definition covers a spectrum from the undulating cilium of many protists and the undulating–rotating cilium of sperm cells to the planar cilium of vertebrate multiciliated cells. In agreement with other zoologists, we reserve the term flagellum for simpler structures found in bacteria, which lack microtubules] bearing a set of proacrosomal vesicles rather than a true acrosome at the anterior pole, and ontogenetically derived from a monociliated rather than a non-ciliated spermatogonium. These spermatozoa are typically found in many lower invertebrates with external fertilization (i.e. ectaquasperms, *sensu* Rouse & Jamieson, 1987). Therefore, external fertilization mediated by such simple spermatozoa has been postulated to represent the ancestral condition in

*Corresponding author. E-mail: maldonado@ceab.csic.es

animals (Franzén, 1956; Afzelius, 1972, 1979; Baccetti & Afzelius, 1976; Reunov, 2001). Given that sponges (phylum Porifera) are accepted by most – although not all – authors to be at the basis of the phylogenetic tree of animals, one should expect simple spermatozoa in this phylum. Among the three classes of Porifera, demosponges are the best studied group in terms of spermatozoon structure. To our knowledge, there is only one transmission electron microscopy (TEM) study addressing the ultrastructure of spermatogenesis for the class Calcarea (Anakina & Drozdov, 2001). Likewise, a brief TEM description of early spermatogenetic stages in the species *Oopsacas minuta* Topsent (Boury-Esnault *et al.*, 1999) provides the only contribution for the class Hexactinellida. The set of available data indicates that the expected 'primitive spermatozoon' occurs in a few demosponges belonging to different taxonomic groups (see Reiswig, 1983 and Boury-Esnault & Jamieson, 1999 for reviews).

It was first thought that the absence of acrosome was the rule in sponge spermatozoa. Nevertheless, proacrosomal vesicles, usually regarded to represent the evolutionary step prior to the apparition of the acrosome (e.g. Baccetti, 1979; Franzén, 1996), have been found in some demosponges (Diaz & Connes, 1980; Gaino *et al.*, 1984; Riesgo, Taylor & Leys, 2007a). This is also the dominant condition in the spermatozoon of most cnidarians (Hinsch, 1974). Early studies based on light microscopy vindicated occurrence of an acrosome in some demosponges (Tuzet, 1964; Reiswig, 1970) and some Calcarea (Gatenby, 1927; Tuzet, 1947). Using electron microscopy, an acrosome has been demonstrated to occur in all studied homosclerophorid demosponges (Baccetti, Gaino & Sarà, 1986; Gaino *et al.*, 1986; Boury-Esnault & Jamieson, 1999; Riesgo, Maldonado & Durfort, 2007b). A large, conical acrosome has also been documented by TEM in the calcaronean *Sycon calcaravis* (Hozawa) (Nakamura, Okada & Watanabe, 1998). Consequently, in contrast to the early view that primitive sperms may have arisen independently in the Porifera and Eumetazoa (Afzelius, 1972; Franzén, 1996), it has now been suggested that the spermatozoon is homologous in all Metazoa (e.g. Mohri, Kubo-Irie & Irie, 1995) and that the absence of acrosome in most sponges could be a derived condition (Baccetti *et al.*, 1986; Harrison & De Vos, 1991; Boury-Esnault & Jamieson, 1999; Riesgo *et al.*, 2007b). In addition, cone-shaped and relatively lengthened sperms, which depart from the archetype of classical primitive sperm (*sensu* Reunov, 2005), have preliminarily been described for members of various demosponge families (Reiswig, 1983; Boury-Esnault & Jamieson, 1999; Riesgo *et al.*, 2007a). A bizarre V-shaped spermatozoon has also been described in the halichondriid *Halichondria panicea* (Pallas) (Barthel & Detmer, 1990). Yet, the most atypical spermatozoon known in demosponges so far belongs to the poecilosclerid *Crambe crambe* (Schmidt). It shows V-shaped morphology and a cilium inserted within a deep cytoplasmic pit (Tripepi, Longo & Camera, 1984). Unfortunately, this distinct sperm was described only in a very brief report included in the Abstracts book of the 8th European Congress of Electron Microscopy. As was noticed by Boury-Esnault & Jamieson (1999) in their review of the poriferan sperm, many of the peculiar ultrastructural traits originally mentioned in that brief preliminary description remain intriguing and need further investigation. In this study, we have revisited the spermatozoon of *C. crambe* in an attempt to gain a better understanding of both the formation process that leads to such unconventional V-shaped morphology and the ultrastructure of the mature spermatozoon. The findings provide elements to revise current hypotheses on both early evolution of spermatozoa and reproductive biology of sponges.

MATERIAL AND METHODS

Sampling

We studied a large *C. crambe* population established on the sublittoral rocky bottoms of the north-eastern Mediterranean coast of Spain (for further information, see Maldonado *et al.*, 2005). To conduct a general monitoring of reproductive activity in the population, we tagged five large and presumably mature individuals, which were sampled monthly from October 2003 to October 2005. Using scuba equipment and surgical scissors, we collected a small piece of tissue (*c.* $1 \times 0.5 \times 0.3$ cm) from each sponge at each sampling time. In no case over the study period did the collection involve dead tissue or perceptible signs of illness in the sponges. During the first year of study, when samples from the tagged individuals revealed that gametogenetic activity was peaking in the population (i.e. late spring to mid summer), we increased both the number of tagged individuals (25 individuals) and sampling frequency (*c.* 10-day intervals).

Light microscopy

Tissue samples were maintained in ambient seawater for transportation to the laboratory and fixed within 2 h after collection. Samples were prepared for light microscopy following the protocol detailed in Riesgo *et al.* (2007b). Sections were studied through a Zeiss Axioplan II compound microscopy connected to a Spot Cooled Color digital camera. We estimated the

number of cyst-producing sponges in the population over time by taking two pictures (6.96 mm^2) of each of two non-serial histological sections per individual and sampling time. Pictures were taken at least 240 μm from each other to avoid overestimation as a result of overlapping of cysts. Then, we used the public domain ImageJ Software (http://rsb.info.nih.gov/ij/index.html) on the digital histological images to estimate the percentage of tissue occupation by cysts, measuring maximum diameter and cyst area per area unit of tissue in the reproductive individuals. Although cysts were usually subspherical, such measurements provided only a relatively approximate assessment of tissue occupancy because all cysts in a section are not caught at their maximum diameter. Nevertheless, because we studied a total of *c*. 550 sections, we assumed that parametric statistics work and that measured mean values are reliable, although affected by a large (non-natural) standard deviation (SD) artificially increased by the position of the sectioning plane in the cyst.

Transmission electron microscopy

The ultrastructure of spermatogenesis was documented using TEM. To capture the various cell stages during the process, tissue samples were collected in May and June of 2004 and July 2005. Samples were fixed within 1 h after collection and then prepared for electron microscopy following the protocol detailed in Riesgo *et al.* (2007b). Observations were conducted with a JEOL 1010 TEM operating at 80 kV and provided with a Gatan module for acquisition of digital images.

RESULTS

Dynamics of cyst production

We examined histological sections of a total of 80 individuals during the 2-year monitoring (October 2003–September 2005). Spermatic cysts occurred in *c*. 50–60% of individuals in the population for *c*. 3 months each year, from late spring to early summer (Fig. 1A). During 2004, cysts appeared in May, but the following year they appeared 1 month earlier (in April). In both years, cysts appeared at the same time as the seasonal rise of seawater temperature. In contrast, they disappeared gradually from the sponge mesohyl during summer (Fig. 1A). Cyst size did not change substantially over the reproductive period, with the average maximum diameter per month ranging from 49.18 ± 36.02 to 65.94 ± 56.46 μm during 2004 and from 46.34 ± 9.05 to 78.76 ± 46.55 μm during 2005 (Fig. 1B).

Tissue occupation by cysts over the spermatogenic cycle was 1.70% on average. The highest values occurred in June 2004 (0.98%) and in May 2005 (5.53%), with sponges making a much higher investment in cyst production per area unit of tissue the latter year (Fig. 1C). Each year, we detected some individuals with quite high cyst production (4–10% of tissue occupation), individuals with low cyst production (< 0.01%) and individuals showing no reproductive activity at all. Individuals with high production in 2004 did not necessarily have high production in 2005 and vice versa. Tagged individuals that did not

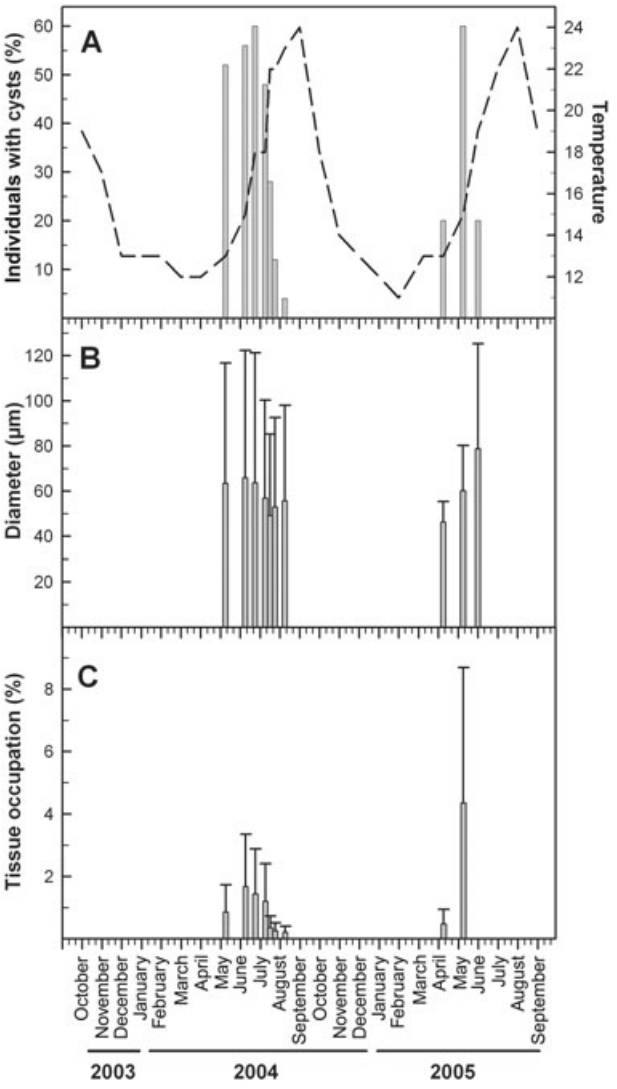

Figure 1. Dynamics of spermatogenesis over a 2-year period. A, percentage of individuals engaged in spermatic cyst production in the population over time plotted vs. seawater temperature. B, time dynamics of cyst size (mean ± SD). C, tissue occupation (%) by cysts. Number of individuals sampled and sampling frequency increased from five to 25 individuals and from 1-month to 10-day intervals in summer 2004, respectively.

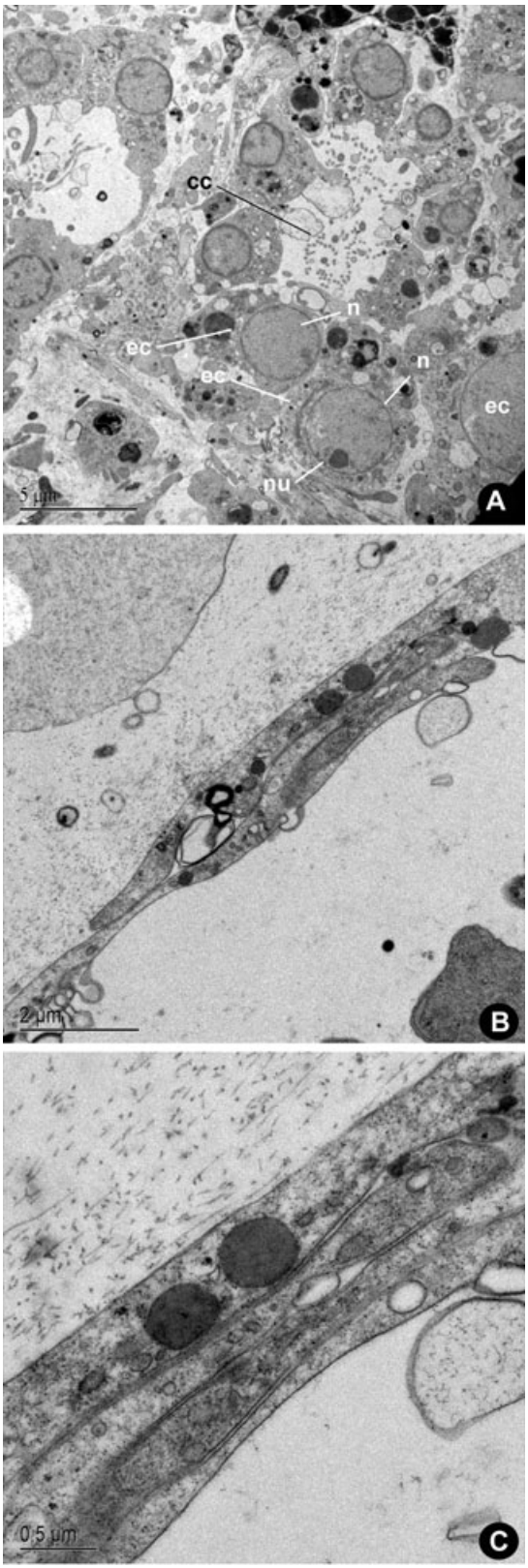

Figure 2. Early spermatogenesis stages. A, choanocyte chamber showing a transition gradient from 'regular' choanocytes to abnormally large choanocytes (ec) with swollen nuclei (n), which are leaving the chamber (cc) to become spermatogonia. Note the nucleolus (nu) in one of the enlarged choanocytes. B–C, interdigitate junctions in the cellular follicle of the spermatic cyst.

reproduce in 2004 did not reproduce the following year either.

Ultrastructure of cysts formation

Spermatogonia derived from choanocytes, as revealed by observations of choanocytes that doubled their nuclear size (mean diameter 4.15 µm) and cell size (6.12 µm in mean height and 5.76 µm in mean width). Such 'swollen' choanocytes were captured in some sections in the process of disassembling their collar and leaving the chambers (Fig. 2A). Prior to transdifferentiation, choanocytes measured 3.5 µm on average in height and 3.2 µm on average in width. Although not all the steps of the initial sequence of spermatic cyst formation were found in our TEM sections, the observations gathered suggest that entire chambers do not transform into cysts. Rather, some swollen choanocytes from different chambers appeared to migrate to the mesohyl for subsequent re-aggregation. Additional research is required to elucidate the details of these initial steps. Early cyst stages were rapidly enveloped by a cellular follicle of unascertained origin (Figs 2A, 3A). The epithelium-like follicle was built by flattened cells with a prominent round nucleus, which connected with each other by interdigitate junctions (Figs 2B, C, 3C, 4A).

The first cysts appeared in the deepest mesohyl region, close to the basopinacoderm, while late cysts occupied the remaining upper mesohyl regions, intermingled with functional choanochambers. Each cyst often contained all cells at the same stage of spermatogenesis, i.e. within-cyst synchronous development (Figs 3A, 4A, 5A). However, there was between-cyst asynchrony, with adjacent cysts often being in different stages of development (Fig. 3C).

Ultrastructure of spermatogonia and primary spermatocytes

Early stage cysts were densely packed with cells, usually consisting of both spermatogonia and primary spermatocytes (Fig. 3A). They were both round monociliated cells (*c*. 5 µm in diameter), showing a large nucleus (4–4.5 µm in diameter), the Golgi apparatus,

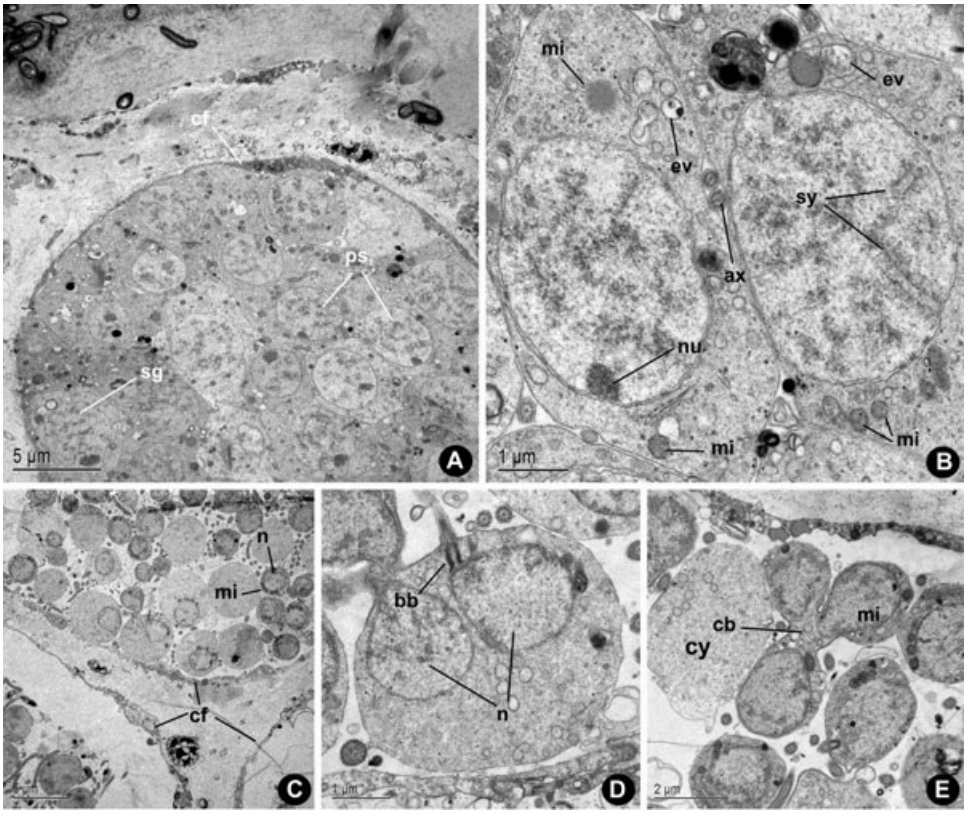

Figure 3. Spermatogonia and primary spermatocytes. A, spermatic cyst containing both spermatogonia (sg) and primary spermatocytes (ps). A cellular follicle (cf) envelops the cyst. B, a spermatogonium (to the right) showing a nucleolate nucleus (n) and a primary spermatocyte with synaptonemal complexes (sy). The cytoplasm of both cells contains several mitochondria (mi) and electron-clear vesicles (ev). Cross-sections of axonemes (ax) occur intercellularly in the cyst. C, three adjacent spermatic cysts containing primary spermatocytes (ps) and enveloped by a cellular follicle (cf). Late primary spermatocytes show a reduced nucleus (n) compared with earlier stages, also an ordered arrangement of the mitochondria (mi). D, primary spermatocyte approaching the cytokinesis of the first meiotic division, in which two nuclei (n), the basal body (bb) and the cilium are seen. E, primary spermatocytes interconnected by a cytoplasmic bridge (cb). Note the arrangement of mitochondria (mi) around the nuclei. Excess cytoplasm (cy) is exocytosed by primary spermatocytes to the cyst lumen.

mitochondria with well-defined, flattened cristae, and several inclusions and electron-clear vacuoles of uncertain nature (Fig. 3A). Nevertheless, spermatogonia were distinguishable from spermatocytes by having a large nucleolus (Fig. 3A). In contrast, primary spermatocytes showed a nucleus with synaptonemal complexes, indicating that they were in prophase I (Fig. 3A, B). As spermatogenesis advanced, cysts became laxer, with primary spermatocytes clearly outnumbering spermatogonia. Primary spermatocytes started reducing their nuclear size (Fig. 3C, D), then also their cell size, by exocytosing part of their cytoplasm (Fig. 3E). At this late stage, several small round mitochondria occurred in a highly ordered distribution around the nucleus (Fig. 3C, E). After nuclear division (Fig. 3D), late-stage primary spermatocytes underwent incomplete cytokinesis, with daughter cells (i.e. secondary spermatocytes) remaining interconnected by cytoplasmic bridges (Fig. 3E).

Ultrastructure of secondary spermatocytes

Secondary spermatocytes were round, monociliated cells, *c*. 2.5 µm in diameter (Fig. 4B). They engaged in a process of chromatin condensation, which started at the inner side of the nuclear membrane and became particularly evident at the area adjacent to the cilium insertion, where a transient nucleolus-like structure appeared (Fig. 4B, D). At the cilium insertion, the basal body (or principal centriole) and a perpendicular accessory centriole were patent (Fig. 4B, D). The cytoplasm contained electron-clear vacuoles and a well-developed Golgi apparatus (Fig. 4C, E).

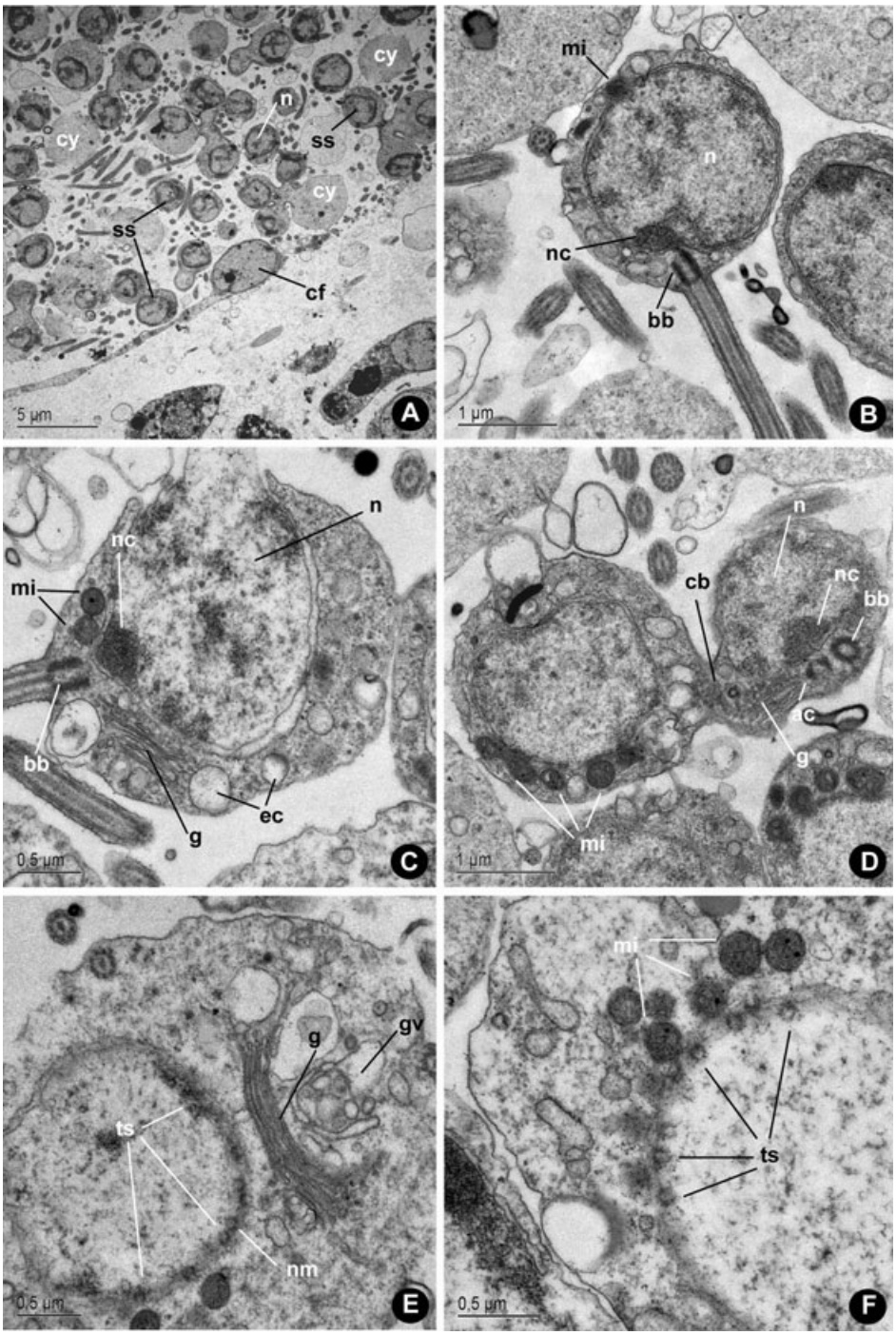

Figure 4. Secondary spermatocytes. A, spermatic cyst containing secondary spermatocytes (ss) with incipient condensation of chromatin in their nucleus (n) and limited by a cellular follicle (cf). Note production of cytoplasmic drops (cy) resulting from the cytoplasmic reduction of the first meiotic division. B–D, secondary spermatocytes showing a peripheral, 'nucleolus-like' condensation of chromatin (nc) in the nucleus (n), the basal body (bb), the accessory centriole (ac), some electron-clear vesicles (ec), mitochondria (mi) and a Golgi apparatus (g). Cytoplasmic bridges (cb) interconnect sister cells. E, nucleus of a secondary spermatocyte showing tube-like structures (ts) at the inner nuclear membrane (nm). A well-developed Golgi apparatus (g) starts producing the vesicles (gv) that will originate the acrosome. F, close-up of a spermatocyte's nucleus showing the intranuclear tube-like structures (ts) and the highly ordered arrangement of mitochondria (mi) around the nuclear envelope.

The small mitochondria maintained their ordered arrangement around the nuclear membrane (Fig. 4D, F). Interestingly, several small, electron-dense tube-like structures appeared at the internal side of the nuclear membrane, just in front of the mitochondria (Fig. 4E, F). During the second meiotic division, secondary spermatocytes exocytosed most of their cytoplasm in the form of large electron-clear drops (Fig. 5A, B). As a result, the cyst appearance became quite lax.

Ultrastructure of spermatids

Spermatids experienced a drastic change in morphology relative to spermatocyte stages. They became lengthened cells, being 5.5 μm long and 1.7 μm wide on average. The nucleus stretched along the longitudinal axis, achieving a length of up to 4.5 μm and narrowing up to 0.5 μm in width (Fig. 5C). Chromatin compaction involved a peculiar process of 'multipolar' condensation, forming small, electron-dense clumps ('initiation centres') which were scattered all over the nucleus (Fig. 5C, F, G). A longitudinal cytoplasmic tunnel, running from the cilium insertion (i.e. the original posterior cell pole) to the anterior cell pole, was formed to harbour the proximal region of the cilium axoneme (Fig. 5D, F). Therefore, the cilium bent at a 180° angle (Fig. 5D, F). As a result, the cell became V-shaped, with the cilium becoming free for beating near the original anterior pole of the spermatid (Fig. 5F), which apparently turned into the new functional posterior pole of the future spermatozoon. The cilium showed a typical 9 + 2 microtubule structure, with alar sheets and anchoring points at the transition region between the axoneme and the basal body (Fig. 5L). The accessory centriole was not visible at this stage, probably having been disassembled. The several mitochondria occurring at previous stages fused into a large single mitochondrion that migrated to the cell pole opposite the cilium insertion (Fig. 5C–E). It is also worth noting the formation of striated ciliary rootlets, which arose from a terminal plate of the basal body (Fig. 5K) and extended to contact the mitochondrion located at the opposite cell pole, running between the nuclear membrane and the cytoplasmic tunnel (Fig. 5F–J). The electron-dense bands of the rootlet were 40 nm wide, being separated by electron-clear, 53-nm wide bands. In early spermatids, the Golgi apparatus, which located at the original anterior pole adjacent to the newly formed mitochondrion (Fig. 5E), produced a large vesicle (Fig. 5E, J). In late spermatids, this vesicle migrated to the new functional anterior pole and began differentiating into an electron-dense acrosomal complex (Fig. 5F, K, L). Occurrence of microtubules in the cytoplasmic bridges between spermatids was another trait not observed at previous stages (Fig. 5C, J).

Ultrastructure of spermatozoa

We never observed free-swimming spermatozoa, but we did observe nearly mature stages sharing the cysts with some late spermatids still exocytosing part of their cytoplasm (Figs 5A, 6A). Intercellular bridges did not occur between those nearly mature spermatozoa. The other major difference with spermatids was that the earlier chromatin clumps condensed into a single helical structure in the spermatozoa (Fig. 6A–C). Spermatozoa were long and narrow monociliated cells, with cell bodies averaging 6.5 μm in length and 0.6 μm in width (Figs 6A, C, 7A). There was neither Golgi apparatus nor accessory centriole. The proximal region of the cilium ran within a cytoplasmic tunnel (Fig. 6A–D) until about the mid point of cell length, where it became free (Fig. 6A). Longitudinal sections showed that the axis of the free-beating axoneme often crossed the longitudinal axis of the cell body (Figs 6C, 7A). As in spermatids, the striated rootlets arising from the basal body ran longitudinally through the entire cell to contact the single mitochondrion located at the opposite pole (Fig. 6C). More importantly, an acrosomal complex formed at the new functional anterior pole. It consisted of an electron-dense, membrane-bound, conical acrosome (Fig. 6A, D, E) and an electron-dense acrosomal rod (Fig. 6D, E) located between the acrosome and the nucleus, adjacent to the basal body. Some sections also revealed that a small vesicle, characterized by a six-layer membrane, surmounted the acrosome and protruded the cell membrane (Fig. 6E, F).

DISCUSSION

Early stages of spermatogenesis in *C. crambe* (i.e. spermatogonia and spermatocytes) closely attached to the pattern described for most other demosponges (e.g. Fell, 1974; Simpson, 1984; Boury-Esnault & Jamieson, 1999), including derivation of monociliated spermatogonia from choanocytes. Nevertheless, spermiogenesis strongly departed from what would be expected to occur in not only demosponges but also other lower metazoans. At the spermatid stage, the formation of a deep ciliary pit to harbour the cilium insertion and a long portion of the proximal axoneme produced a V-shaped spermatozoon similar in general organization to that known in some phoronids (Fig. 7F; e.g. Franzén & Ahlfors, 1980; Zimmer, 1991; Reunov & Klepal, 2004). While it has been suggested that such a cytoplasmic tunnel is formed in *Phoronopsis harmeri* Pixel by migration of the ciliary basal

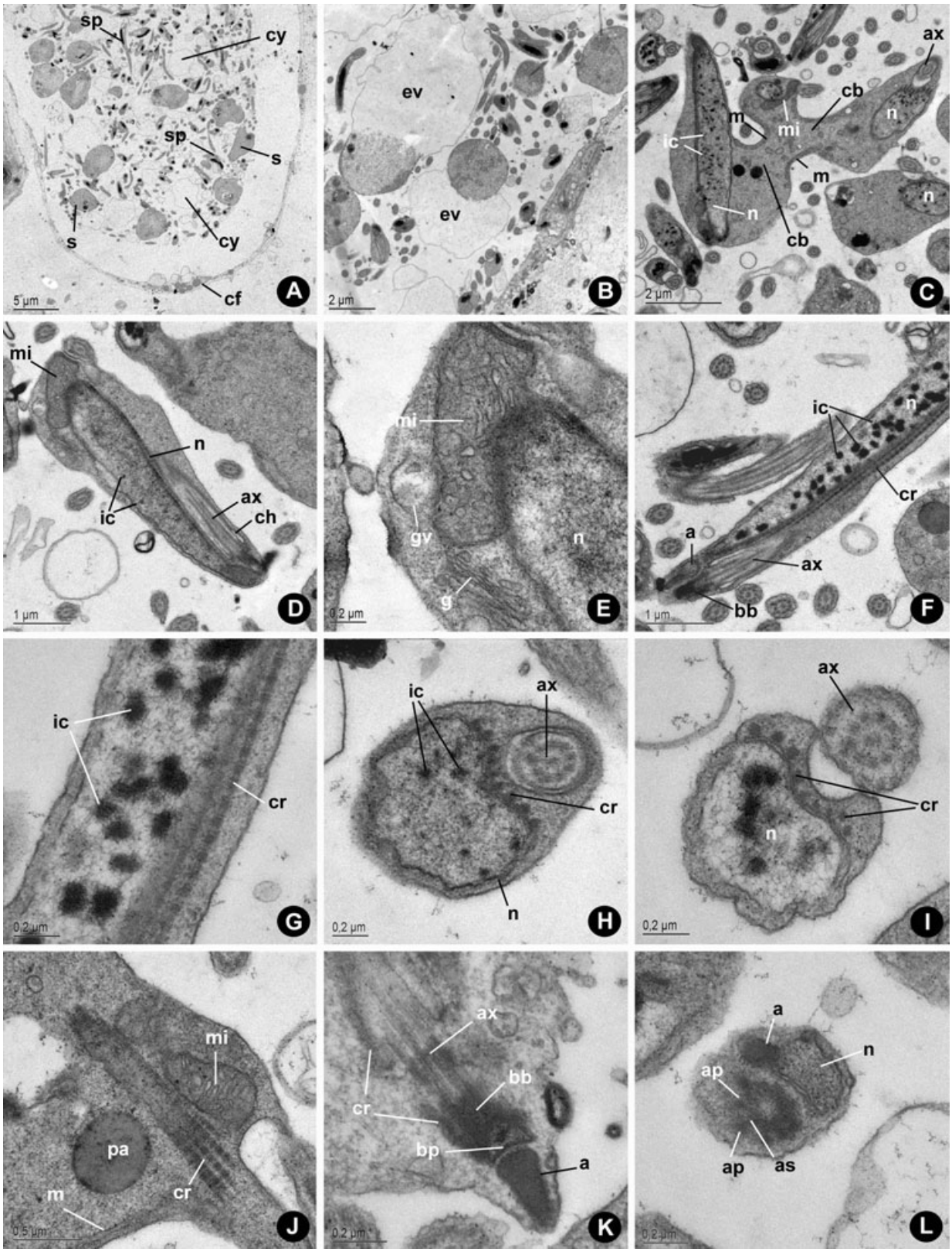
sp
cy
sp
s
s
cy
cf
5 µm
A
ev
ev
2 µm
B
ax
cb
n
m
mi
ic
m
n
n
cb
2 µm
C
mi
n
ax
ic
ch
1 µm
D
mi
gv
n
g
0,2 µm
E
ic
n
cr
a
ax
bb
1 µm
F
ic
cr
0,2 µm
G
ic
ax
cr
n
0,2 µm
H
ax
cr
n
0,2 µm
I
mi
pa
m
cr
0,5 µm
J
ax
bb
cr
bp
a
0,2 µm
K
a
n
ap
ap
as
0,2 µm
L

Figure 5. Spermatids. A, spermatic cyst limited by a cell follicle (cf) and containing spermatids (s) and mature spermatozoa (sp). Intercellular electron-clear vacuoles result from processing of cytoplasmic drops (cy). B, spermatids exocytosing large electron-clear vacuoles (ev) with cytoplasm excess. C–D, spermatids with lengthened nucleus (n) showing multiple 'initiation centres' (ic) of chromatin condensation, the cytoplasmic tunnel (ct) lodging the axoneme (ax) and the newly formed single mitochondrion (mi). Note that sister spermatids (C) are connected by cytoplasmic bridges (cb) reinforced by microtubules (m). E, detail of the functional posterior pole showing the mitochondrion (mi), the nucleus (n) and a putative 'proacrosomal' vesicle (gv) produced by the Golgi apparatus (g). F–G, longitudinal sections of spermatids showing the axoneme (ax), the striated ciliary rootlets (cr) and the nucleus (n) with multiple 'initiation centres' (ic). A developing acrosomal complex (a) occurs close to the basal body (bb). H, spermatid cross-sectioned near the level of the cilium insertion showing 'initiation centres' (ic) in the nucleus (n), ciliary rootlets (cr) associated with the external nuclear membrane and the cytoplasmic tunnnel that harbours the axoneme (ax). I, spermatid cross-sectioned at its mid length showing the ciliary rootlets (cr) and the free-beating axoneme (ax) before entering the cytoplasmic tunnel. J, detail of striated ciliary rootlets (cr) in close association with the mitochondrion (mi). Note the migrating 'proacrosomal vesicle' (pa) and the microtubules (m) reinforcing the plasmalemma at the inter-spermatid bridges. K, detail of a spermatid showing the insertion of the axoneme (ax), the basal body (bb) with a terminal plate (bp) from which ciliary rootlets (cr) originate and the conical acrosome (a). L, Cross section of a spermatid at the basal body level in which alar sheets (as) and anchoring points (ap) can be inferred. The incipient acrosomal complex (a) and the nucleus (n) are also seen.

body from the posterior to the anterior cell pole (Reunov & Klepal, 2004), our observations suggest that rather it forms in *C. crambe* because the cytoplasm stretches around the proximal portion of the cilium. It is also worth noting that, in addition to *C. crambe*, the spermatozoon of several spongillids, such as *Lubomirskia baikalensis* (Efremova & Papkovskaya, 1980), *Ephydatia fluviatilis* and *Spongilla lacustris* Linnaeus (Paulus, 1989) and the poecilosclerid *Asbestopluma occidentalis* (Riesgo *et al.*, 2007a) also posseses a relatively deep cytoplasmic pit (Fig. 7C–E). None of these sponges shows V-shaped sperm. The spermatid of the poecilosclerid *Anchinoe paupertas* (Bowerbank) also possesses a deep ciliary pit but its mature spermatozoon remains uninvestigated (De Vos *et al.*, 1991). Therefore, given the relatively scarce information regarding spermatogenesis and spermatozoa in Porifera, it cannot be ruled out that V-shaped spermatozoa may occur more often than thought in some poecilosclerid subgroups. Interestingly, a V-shaped spermatozoon, but lacking cytoplasmic tunnelling for the cilium (Fig. 7B), occurs in the halichondriid demosponge *Halichondria panicea* (Barthel & Detmer, 1990).

In association with the cilium, we have found well-developed striated rootlets that arise from the basal body and run parallel to the nuclear envelope to reach the mitochondrion located at the opposite cell pole. Such a structure had never been reported in the sperm of other poriferans to date. This rootlet could have a role in reinforcing the anchoring of the cilium, which may require extra support when pushing the V-shaped cell. Nevertheless, they may also participate in energy transference from the mitochondrion to the basal body for ciliary beating, as large mitochondria usually occur in contact with rootlets in many types of cilium-bearing cells in sponges (e.g. Woollacott & Pinto, 1995; Maldonado *et al.*, 2003; Maldonado, 2004).

Another remarkable transformation during spermiogenesis of *C. crambe* is that spermatids elongate substantially, their nucleus stretching accordingly, and its chromatin condenses by a multipolar process into a helical structure. Helically condensed chromatin is known from the modified sperm of some invertebrates, such as phoronids (e.g. Reunov & Klepal, 2004) and octopodan cephalopod molluscs (e.g. Giménez-Bonafé *et al.*, 2002). Helical chromatin compaction is not to be confused with the helical coiling of the elongated nucleus reported in several other invertebrates (e.g. Alberti, 1995; Ferraguti & Balsamo, 1995). Immediately prior to nuclear elongation of *C. crambe* spermatids, tube-like structures (Fig. 4E, F) appear attached to the internal side of the nuclear envelope. We suspect that these structures may be microtubule derived and somehow involved in the process of nuclear stretching. Such structures had never been reported in Porifera. Cytoplasmic rather than nuclear microtubules have occasionally been regarded to be involved in stretching and helicoidally coiling of the sperm nucleus in other poecilosclerid (Riesgo *et al.*, 2007a) and several invertebrates (e.g. Giménez-Bonafé *et al.*, 2002). Cytoplasmic microtubules also occurred, reinforcing the internal side of the plasmalemma in the inter-spermatid bridges (Fig. 5C, J), and have been previously described in the intercellular bridges that connect the photoreceptory cells of some demosponge larvae (Maldonado *et al.*, 2003).

The presence of a subacrosomal rod in *C. crambe*, which according to its appearance and position appears to be homologous to the axial rod (= perforatorium) known from the sperms of most invertebrates and vertebrate animals, is also noteworthy. To date,

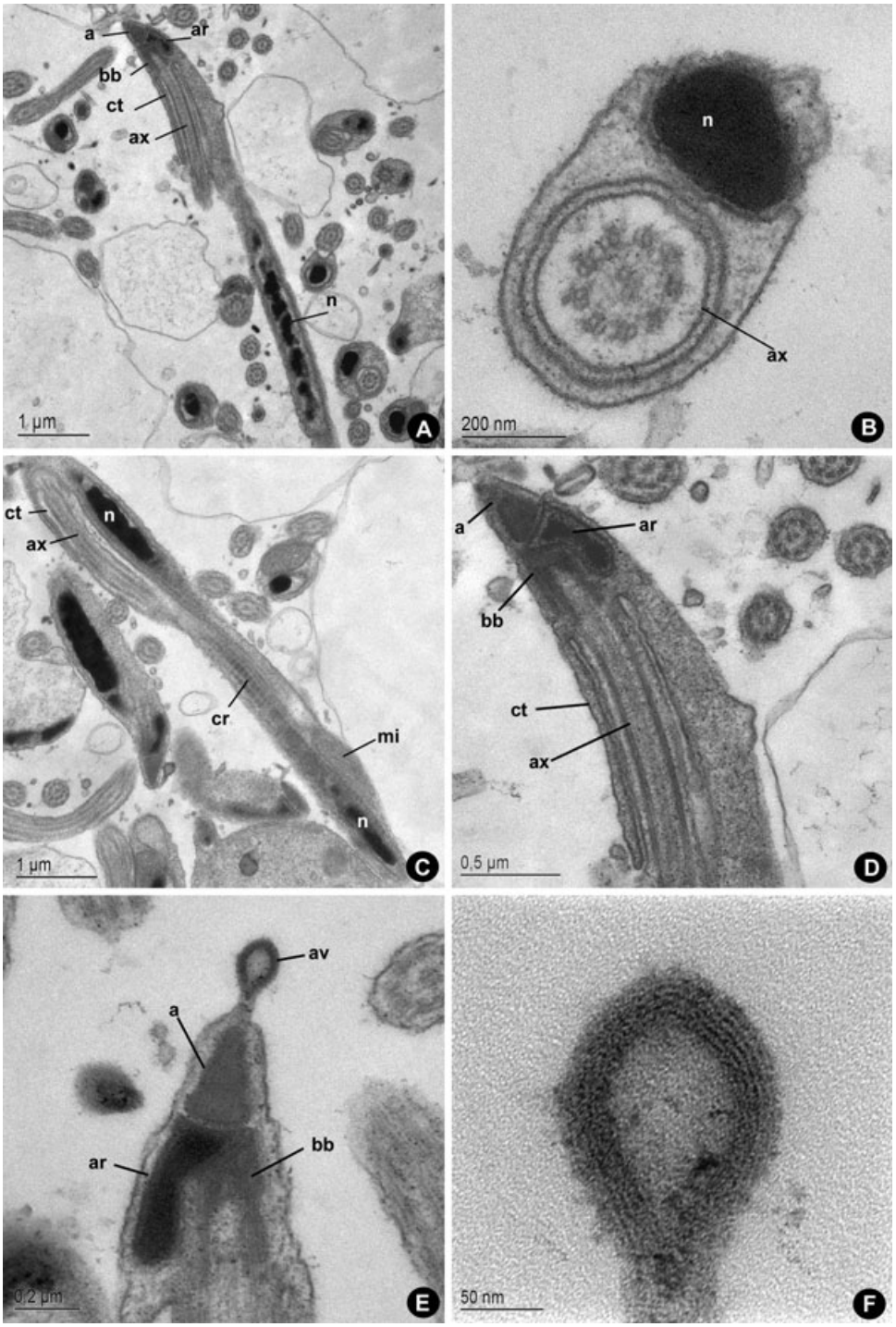

Figure 6. Mature spermatozoa. A, longitudinal section of a spermatozoon showing the helical arrangement of the chromatin in the nucleus (n), the acrosome (a), the acrosomal rod (ar), the basal body (bb) and the cytoplasmic tunnel (ct). B, cross section of a spermatozoon showing the axoneme (ax) within the cytoplasmic tunnel. Note the typical 9 + 2 organization of the axoneme. C, longitudinal section of a spermatozoon showing the nuclear ends (n), the cilium insertion within the cytoplasmic tunnel (ct) and the tendency of the axoneme (ax) to cross the longitudinal axis of the cell body (see Fig. 7A). Long striated rootlets (cr) and the single mitochondrion (mi) are also patent. D, longitudinal section at the acrosomal cell pole showing the cytoplasmic tunnel (ct) lodging insertion of the axoneme (ax), a conical acrosome (a) located adjacent to the acrosomal rod (ar) and the basal body (bb). E–F, detail of the conical acrosome (a) and the acrosomal rod (ar). A vesicle (av) characterized by a complex, multilayered membrane surmounts the acrosome.

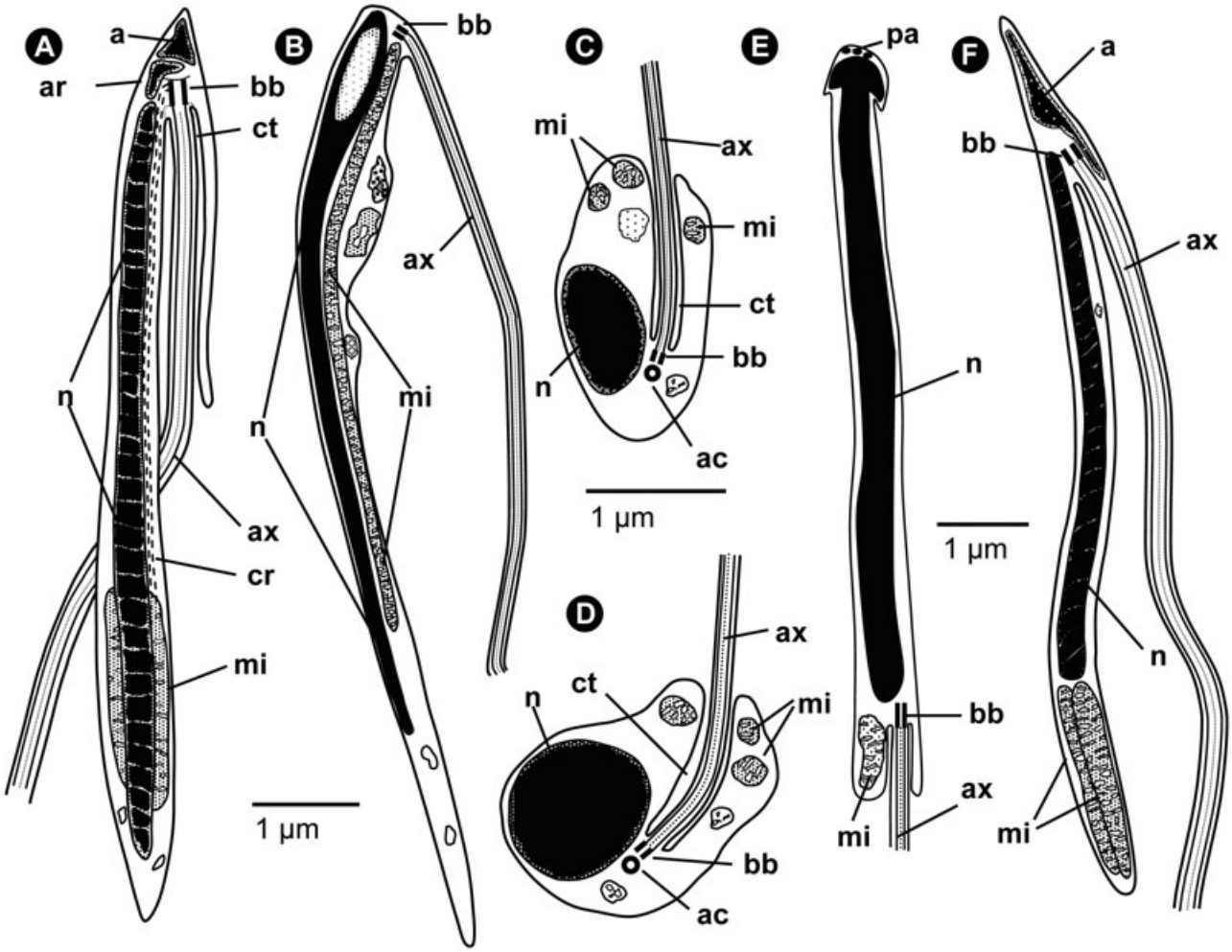

Figure 7. Schematic diagram summarizing the ultrastructure of both several unconventional demosponge spermatozoa and the spermatozoon of the phoronid *Phoronopsis harmeri.* A, V-shaped spermatozoon of the poecilosclerid *Crambe crambe*. B, V-shaped sperm of the halichondriid *Halichondria panicea* (see Barthel & Detmer, 1990). C–D, spermatozoa of the haplosclerids *Spongilla lacustris* (see Paulus, 1989) and *Lubomirskia baikalensis* (see Efremova & Papkovskaya, 1980). E, elongated spermatozoon of the poecilosclerid *Asbestopluma occidentalis* (see Riesgo *et al.*, 2007a). F, V-shaped spermatozoon of the phoronid *P. harmeri* (see Reunov & Klepal, 2004). a, acrosome; ac, accessory centriole; ar, acrosomal rod; ax, axoneme; bb, basal body; ct, cytoplasmic tunnel; cr, ciliary rootlets; mi, mitochondrion; n, nucleus; pa, proacrosomal vesicles.

ctenophores and nemerteans were thought to be the 'lowest' metazoan groups possessing a well-developed acrosome with subacrosomal rod (Franzén, 1987). Although the axial rod of spermatozooa was originally regarded as a structure designed to pierce the egg membranes mechanically, the modern view is that this proteinaceous structure is a cytoskeletal piece that anchors the proximal region of the acrosome to the nuclear membrane below. To date, no other sponge spermatozoon has been reported to have a subacrosomal rod. Another unprecedented feature is the small vesicle, characterized by a multilayer–layer membrane that surmounts the acrosome (Fig. 6E, F).

Our ultrastructural findings are largely consistent with the brief but excellent study by Tripepi *et al.* (1984), in which many of the striking features of the spermatozoon of *C. crambe* were formerly outlined. One discrepancy is the two electron-dense 'basal rods' of unknown function, which, along with the mitochondrion, were reported to flank the nucleus and have not been found in our study.

The available evidence to date strongly supports the view that, unlike that expressed in most general reviews on sperm evolution, the spermatozoa of demosponges can be classified as belonging to two structural types, i.e. 'primitive' and 'derived or modified'

(*sensu* Reunov, 2005), depending on the taxa. Such a situation is similar to that which is known in many protostomes (e.g. Afzelius, 1979; Ying *et al.*, 2004) and a few deuterostome groups (e.g. Afzelius, 1972). The evolutionary significance of this sperm duality in Porifera is intriguing. Because V-shaped and elongated spermatozoa with elongated nucleus are widely regarded as a 'derived' character condition (e.g. Franzén, 1987; Reunov, 2005), one should conclude that co-occurrence of 'primitive' and 'derived' spermatozoa is a situation established in the Porifera prior to the emergence of higher metazoans. Otherwise, occurrence in Porifera of 'derived' spermatozoa that share many ultrastructural traits with those of higher metazoans could only be explained by multiple cases of convergent evolution. This would require embracing the little parsimonious hypothesis of multiple independent inventions by different animal phyla of nearly identical acrosomal vesicles and perforatoria, machineries for cell and nuclear elongation, etc.

However, it has been long postulated that the shape of the spermatozoon is influenced by not only phylogenetic relationships but also physiological and functional demands during dispersal and fertilization (e.g. Franzén, 1956; Afzelius, 1979; Rouse & Jamieson, 1987). From this functional perspective, the hermaphroditic sperm-casting (*sensu* Bishop & Pemberton, 2006) demosponge *C. crambe* produces spermatozoa belonging to the 'entaquaspermatozoon' type, i.e. modified spermatozoa that are released to the seawater by male-acting individuals and subsequently taken by female-acting conspecifics (Rouse & Jamieson, 1987). In sperm-casting sponges (*sensu* Bishop & Pemberton, 2006), the assumed sequence of events leading to internal fertilization can be summarized in three steps: (1) choanocytes of the female-acting individuals engulf free-swimming spermatozoa that entered the body with the inhalant seawater flow; (2) these choanocytes disassemble their cilium and collar microvilli and leave the choanochambers as amoeboid cells (i.e. carrier cells), carrying the spermatozoon within a non-digestive vesicle, the spermiocyst; (3) carrier cells find oocytes nested in the sponge mesohyl and transfer the spermiocyst to them.

Although for carnivorous demosponges an alternative mechanism has been proposed to explain internal fertilization in the absence of aquiferous system and choanocytes (Riesgo *et al.*, 2007a), mediation of carrier cells is the mechanism assumed for internal fertilization in all the remaining (i.e. choanocyte-bearing) demosponges (e.g. Harrison & De Vos, 1991). Nevertheless, a glance at the scientific literature reveals that the participation of carrier cells is only well documented in fertilization of sponges belonging to the class Calcarea (e.g. Simpson, 1984; Harrison & De Vos, 1991; Nakamura *et al.*, 1998). The participation of carrier cells in demosponge fertilization was originally suggested by light microscopy approaches (e.g. Tuzet, 1930; Tuzet & Paris, 1964). Surprisingly, participation of carrier cells in demosponge fertilization has not, so far, been corroborated by TEM. There is only the exception to the recent description of a putative – but not fully confirmed – carrier cell leaving a choanochamber in the homosclerophorid *Corticium candelabrum* Schmidt (Riesgo *et al.*, 2007b). If no carrier cell was to act in sperm transmission in *C. crambe*, the 'V' shape could be interpreted as a morphological design addressed to enhance the spermatozoon progression through the various sponge epithelia and the mesohyl, a collagen-rich medium far more viscous than seawater. A spermatozoon attempting to swim forward in such a dense medium would require enhanced rotation capabilities to deal with viscosity. We postulate that the reason why the proximal portion of the axoneme does not run parallel to the longitudinal axis of the sperm head, but crosses it (Fig. 7A) – as was also depicted by Tripepi *et al.* (1984), is that such an arrangement favours rotation of the whole V-shaped sperm when moving forward. The short arm of the V-shaped structure, i.e. the sperm head, appears to be designed to stabilize the gravity centre during rotation, counterbalancing the pushing of the cilium. The remarkable striated rootlet in the spermatozoon may also have developed to cope with the additional requirements in terms of energy supply and anchorage that ciliary beating into a very viscous medium may demand. Likewise, if no carrier cell were to be involved in sperm transfer, the presence of a complex acrosomal system to enter the oocyte would be justified. This situation is expected to affect not only *C. crambe*, but also many other internally fertilizing demosponges, particularly those in the order Poecilosclerida.

ACKNOWLEDGEMENTS

The authors thank Carmen Carmona, Sergio Taboada, Laura Núñez, Henar Cuervo and David Costalago for their help in either field work or sample processing. We also thank Nùria Cortadellas and Almudena García for their valuable assistance with the TEM sample processing. The research was supported by two grants from the Spanish Ministry for Science and Education (MEC-CTM2005-05366/MAR; MCI-BFU2008-00227/BMC). The work conducted in this study complies with the current laws of Spain.

REFERENCES

Afzelius B. 1972. Sperm morphology and fertilization biology. In: Beatty R, Gluecksohn-Waelsch S, eds. *Proceedings of the international symposium of the genetics of the spermatozoon*. EdInburgh and New York: Bogtrykkeriet Forum, 131–143.

Afzelius B. 1979. Sperm structure in relation to phylogeny in lower metazoa. In: Fawcett DW, Bedford JM, eds. *The spermatozoon*. Baltimore-Munich: Urban & Schwarzenberg, Inc., 243–251.

Alberti G. 1995. Comparative spermatology of Chelicerata: review and perspective. In: Jamieson BGM, Ausió J, Justine JL, eds. *Advances in spermatozoan phylogeny and taxonomy*. Paris: Mémoires du Muséum National d'Histoire Naturelle, 203–230.

Anakina RP, Drozdov AL. 2001. Gamete structure and fertilization in the Barents Sea sponge *Leucosolenia complicata*. *Russian Journal of Marine Biology* **27:** 143–150.

Baccetti B. 1979. The evolution of the acrosomal complex. In: Fawcett DW, Bedford JM, eds. *The spermatozoon*. Baltimore, Munich: Urban & Schwarzenberg, 305–328.

Baccetti B, Afzelius B. 1976. The biology of the sperm cell. *Monographs in Developmental Biology* **10:** 1–254.

Baccetti B, Gaino E, Sarà M. 1986. A sponge with acrosome: *Oscarella lobularis*. *Journal of Ultrastructure and Molecular Structure Research* **94:** 195–198.

Barthel D, Detmer A. 1990. The spermatogenesis of *Halichondria panicea* (Porifera, Demospongiae). *Zoomorphology* **110:** 9–15.

Bishop J, Pemberton A. 2006. The third way: spermcast mating in sessile marine invertebrates. *Integrative and Comparative Biology* **46:** 398–406.

Boury-Esnault N, Efremova S, Bézac C, Vacelet J. 1999. Reproduction of a hexactinellid sponge: first description of gastrulation by cellular delamination in the Porifera. *Invertebrate Reproduction and Development* **35:** 187–201.

Boury-Esnault N, Jamieson B. 1999. Porifera. In: Adiyodi KG, Adiyodi RG, eds. *Reproductive biology of invertebrates. IX. Progress in male gamete ultrastructure and phylogeny*. Chichester: John Wiley and Sons, 1–20.

De Vos L, Rützler K, Boury-Esnault N, Donadey C, Vacelet J. 1991. *Atlas of sponge morphology*. Washington, London: Smithsonian Institution Press.

Diaz JP, Connes R. 1980. Étude ultrastructurale de la spermatogenèse d'une. *Démosponge. Biologie Cellulaire* **38:** 225–230.

Efremova S, Papkovskaya MV. 1980. Spermatogenesis of the sponge *Lubomirskia baicalensis* (Pallas). Ultrastructural investigation. *Arkiv Anatomii, Gistologii i Ehmbriologii* **12:** 88–95.

Fell P. 1974. Porifera. In: Giese A, Pearse J, eds. *Reproduction of marine invertebrates: acoelomate and pseudocoelomate metazoans*. New York: Academic Press, 51–132.

Ferraguti M, Balsamo M. 1995. Comparative spermatology of Gastrotricha. In: Jamieson B, Ausió J, Justine J, eds. *Advances in spermatozoal phylogeny and taxonomy*. Paris: Mémoires du Muséum National d'Histoire Naturelle, 105–117.

Franzén Å. 1956. On spermiogenesis, morphology of spermatozoon and biology of fertilization among invertebrates. *Zoologiska bidrag från Uppsala* **3:** 355–482.

Franzén Å. 1970. Phylogenetic aspects of the morphology of spermatozoa and spermiogenesis. In: Baccetti B, ed. *Comparative spermatology*. New York: Academic Press, 29–46.

Franzén Å. 1987. Spermatogenesis. In: Giese AC, Pearse JS, Pearse VB, eds. *Reproduction in marine invertebrates*. Pacific Groove, CA: Boxwood Press, 1–47.

Franzén Å. 1996. Ultrastructure of spermatozoa and spermiogenesis in the hydrozoan *Cordylophora caspia*, with comments on structure and evolution of the sperm in the Cnidaria and the Porifera. *Invertebrate Reproduction and Development* **29:** 19–26.

Franzén Å, Ahlfors K. 1980. Ultrastructure of spermatids and spermatozoa in *Phoronis*, Phylum Phoronida. *Journal of Submicroscopical Cytology and Pathology* **12:** 585–597.

Gaino E, Burlando B, Buffa P, Sarà M. 1986. Ultrastructural study of spermatogenesis in *Oscarella lobularis* (Porifera, Demospongiae). *International Journal of Invertebrate Reproduction and Development* **10:** 297–305.

Gaino E, Burlando B, Zunino L, Pansini M, Buffa P. 1984. Origin of male gametes from choanocytes in *Spongia offcinalis* (Porifera, Demospongiae). *International Journal of Invertebrate Reproduction and Development* **7:** 83–93.

Gatenby J. 1927. Further notes on the gametogenesis and fertilization of sponges. *Quarterly Journal of Microscopical Science* **71:** 173–188.

Giménez-Bonafé P, Ribes E, Sautière P, González A, Kasinsky HE, Kouach M, Sautière P-E, Ausió J, Chiva M. 2002. Chromatin condensation, cysteine-rich protamine, and establishment of disulphide interprotamine bonds during spermiogenesis of *Eledone cirrhosa* (Cephalopoda). *European Journal of Cell Biology* **81:** 341–349.

Harrison FW, De Vos L. 1991. Porifera. In: Harrison FW, eds. *Microscopic anatomy of invertebrates*. New York: Wiley-Liss, 29–89.

Hinsch G. 1974. Comparative ultrastructure of cnidarian sperm. *Integrative and Comparative Biology* **14:** 457–465.

Maldonado M. 2004. Choanoflagellates, choanocytes and animal multicellularity. *Invertebrate Biology* **123:** 1–22.

Maldonado M, Carmona M, Velásquez Z, Puig M, Cruzado A, López A, Young C. 2005. Siliceous sponges as a Silicon sink: an overlooked aspect of benthopelagic coupling in the marine Silicon cycle. *Limnology and Oceanography* **50:** 799–809.

Maldonado M, Durfort M, McCarthy DA, Young CM. 2003. The cellular basis of photobehaviour in the tufted parenchymella larva of demosponges. *Marine Biology* **143:** 427–441.

Mohri H, Kubo-Irie M, Irie M. 1995. Outer arm dynein of sperm flagella and cilia in the animal kingdom. *Mémoires Museé Nationale Histoire Naturelle* **166:** 15–22.

Nakamura Y, Okada K, Watanabe Y. 1998. The ultrastructure of spermatozoa and its structural change in the choanocytes of *Sycon calcaravis* Hozawa. In: Watanabe Y, Fusetani N, eds. *Sponge sciences*. Tokyo: Springer Verlag, 179–191.

Nielsen C. 2001. *Animal evolution. Interrelationships of the living phyla*. Oxford: Oxford University Press.

Paulus W. 1989. Ultrastructural investigation of spermatogenesis in *Spongilla lacustris* and *Ephydatia fluviatilis* (Porifera, Spongillidae). *Zoomorphology* **109:** 123–130.

Reiswig H. 1970. Porifera: sudden sperm release by tropical Demospongiae. *Science* **170:** 538–539.

Reiswig HM. 1983. Porifera. In: Adiyodi KG, Adiyodi RG, *Reproductive biology of invertebrates II spermatogenesis and sperm function*. Chichester: John Wiley and Sons Ltd., 1–21.

Reunov A. 2001. Is the 'flagellated' pattern of spermatogenesis plesiomorphic in Metazoa? *Invertebrate Reproduction and Development* **40:** 239–242.

Reunov A. 2005. Problem of terminology in characteristics of spermatozoa of Metazoa. *Russian Journal of Developmental Biology* **36:** 335–351.

Reunov A, Klepal W. 2004. Ultrastructural study of spermatogenesis in *Phoronopsis harmeri* (Lophophorata, Phoronida). *Helgoland Marine Research* **58:** 1–10.

Riesgo A, Taylor C, Leys S. 2007a. Reproduction in a carnivorous sponge: the significance of the absence of an aquiferous system to the sponge body plan. *Evolution and Development* **9:** 618–631.

Riesgo A, Maldonado M, Durfort M. 2007b. Dynamics of gametogenesis, embryogenesis, and larval release in a Mediterranean homosclerophorid demosponge. *Marine and Freshwater Research* **58:** 398–417.

Rouse G, Jamieson B. 1987. An ultrastructural study of the spermatozoa of the polychaetes *Eurythoe complanata* (Amphinomidae), *Clymenella* sp. and *Micromaldane* sp. (Maldanidae). *Journal of Submicroscopical Cytology and Pathology* **19:** 573–584.

Simpson T. 1984. Gamete, embryo, larval development. In: Simpson T, ed. *The cell biology of sponges*. Berlin: Springer Verlag, 341–413.

Tripepi S, Longo O, La Camera R. 1984. A new pattern of spermiogenesis in the sponge *Crambe crambe*: preliminary observations. In: Csanády A, Röhlich P, Szabó D, eds. *Proceedings of the Eighth European Congress on Electron Microscopy*. Budapest: Programme Committee, 2073–2074.

Tuzet O. 1930. Sur la fécondation de l'eponge siliceuse *Cliona viridis* Schmidt. *Comptes Rendus de l'Academie des Sciences, Paris* **191:** 1095–1097.

Tuzet O. 1947. L'ovogenèse et la fécondation de l'éponge calcaire *Leucosolenia* (*Clathrina*) *coriacea* Mont. et de l'éponge siliceuse *Reniera elegans* Bow. *Archives de zoologie expérimentale et génerale* **85:** 127–148.

Tuzet O. 1964. L'origine de la ligneé germinale et la gametogénèse chez les spongiaires. In: Wolff E, ed. *L'origine de la Ligneé Germinale*. Paris: Hermann, 79–111.

Tuzet O, Paris J. 1964. La spermatogenèse, l'ovogenèse, la fécondation et les premiers stades du développement chez *Octavella galangaui*. *Vie et Milieu* **15:** 309–327.

Woollacott R, Pinto R. 1995. Flagellar basal apparatus and its utility in phylogenetic analyses of the Porifera. *Journal of Morphology* **226:** 247–265.

Ying X, Yang W, Jiang N, Zhang Y. 2004. Ultrastructure of spermatozoa of *Bullacta exarata* (Philippi) and its significance on reproductive evolution and physioecological adaptation. *Z Zhejiang Univ SCI* **5:** 1211–1217.

Zimmer R. 1991. Phoronida. In: Giese AC, Pearse JS, Pearse VB, eds. *Reproduction of marine invertebrates*. Pacific Grove: The Boxwood Press, 1–45.